Public Health England

Protecting and improving the nation's health

# NHS Breast Screening Programme Equipment Report

## Technical evaluation of GE Senographe Pristina digital mammography system in 2D mode

December 2019

# About Public Health England

Public Health England exists to protect and improve the nation's health and wellbeing, and reduce health inequalities. We do this through world-leading science, knowledge and intelligence, advocacy, partnerships and the delivery of specialist public health services. We are an executive agency of the Department of Health and Social Care, and a distinct delivery organisation with operational autonomy. We provide government, local government, the NHS, Parliament, industry and the public with evidence-based professional, scientific and delivery expertise and support.

Public Health England, Wellington House, 133-155 Waterloo Road, London SE1 8UG
Tel: 020 7654 8000 www.gov.uk/phe
Twitter: @PHE_uk Facebook: www.facebook.com/PublicHealthEngland

## About PHE screening

Screening identifies apparently healthy people who may be at increased risk of a disease or condition, enabling earlier treatment or informed decisions. National population screening programmes are implemented in the NHS on the advice of the UK National Screening Committee (UK NSC), which makes independent, evidence-based recommendations to ministers in the 4 UK countries. PHE advises the government and the NHS so England has safe, high quality screening programmes that reflect the best available evidence and the UK NSC recommendations. PHE also develops standards and provides specific services that help the local NHS implement and run screening services consistently across the country.

www.gov.uk/phe/screening Twitter: @PHE_Screening Blog: phescreening.blog.gov.uk
For queries relating to this document, please contact: phe.screeninghelpdesk@nhs.net



Published December 2019
PHE publications gateway number:

PHE supports the UN Sustainable Development Goals

# Contents

# Executive summary

The purpose of the evaluation was to determine whether the GE Senographe Pristina meets the main standards in the NHS Breast Screening Programme (NHSBSP) and European protocols, and to provide performance data for comparison against other systems.

The mean glandular dose (MGD) was found to be well below the remedial level for all automatic exposure control (AEC) modes. For the 53mm equivalent standard breast, the MGD was 1.19mGy in Standard mode, compared with the remedial level of 2.5mGy. The image quality, as measured by threshold gold thickness, is at the achievable level for the Standard mode.

The GE Senographe Pristina, operating in 2D mode, meets the requirements of the NHSBSP standards for digital mammography systems.

# 1. Introduction

## 1.1 Testing procedures and performance standards for digital mammography

This report is one of a series evaluating commercially available direct digital radiography (DR) systems for mammography on behalf of the NHS Breast Screening Programme (NHSBSP). The testing methods and standards applied are mainly derived from NHSBSP Equipment Report 0604[1] which is referred to in this document as 'the NHSBSP protocol'. The standards for image quality and dose are the same as those provided in the European protocol,[2,3] but the latter has been followed where it provides a more detailed standard, for example, for the automatic exposure control (AEC) system.

Some additional tests were carried out according to the UK recommendations for testing mammography X-ray equipment as described in IPEM Report 89.[4]

## 1.2 Objectives

The aims of the evaluation were:

- to determine whether the GE Senographe Pristina digital mammography system, operating in 2D mode, meets the main standards in the NHSBSP and European protocols
- to provide performance data for comparison against other systems

# 2. Methods

## 2.1 System tested

The tests were conducted at the GE factory in Buc, Paris, on a GE Senographe Pristina system as described in Table 1. The Pristina is shown in Figure 1.

**Table 1. System description**

| | |
|---|---|
| Manufacturer | GE Healthcare |
| Model | Senographe Pristina |
| System serial number | 000011171069167144 |
| Target material | Molybdenum, rhodium |
| Added filtration | 30µm molybdenum, 30 µm silver |
| Detector type | Caesium iodide with amorphous silicon |
| Detector serial number | J125020 |
| Pixel size | 100µm |
| Detector size | 240mm x 286mm |
| Pixel array | 2294 x 1914, 2850 x 2394 |
| Typical image sizes | 9MB (small field size), 13MB (large field size) |
| Pixel value offset | 0 |
| Source to detector distance | 660mm |
| Source to table distance | 637mm |
| Pre-exposure | Thickness < 38mm : 26kV Mo/Mo 2mAs<br>Thickness 38-65mm: 34kV Rh/Ag, 2mAs<br>Thickness > 65mm: 34kV Rh/Ag, 4mAs |
| AEC modes | Standard, Dose-, Standard+, Implant |
| Software version | 1.13 (latest version is 4.2.39C) |

Four AEC modes are available for use with the Pristina, as listed in table 1. The AEC is referred to by GE as Automatic Optimisation of Parameters (AOP).

Exposure factors 26kV Mo/Mo are used for small breasts, for exposures at up to 35mm radiological thickness, which is defined as the equivalent thickness of polymethyl methacrylate (PMMA) plus 2mm or 5%. For thicker breasts the factors used are 34kV Rh/Ag. The mAs is selected as appropriate for the most dense part of the breast. 29kV Mo/Mo is used for exposures of smaller thicknesses when the magnification table is in use.

## 2.2 Output and HVL

An ion chamber was used to measure the output and half-value-layer (HVL), as described in the NHSBSP protocol, at intervals of 3kV. Tube voltage was measured with a RMI 232 kV meter, which was only calibrated for Mo/Mo exposures.

**Figure 1. The GE Senographe Pristina**

## 2.3 Detector response

The detector response was measured as described in the NHSBSP protocol, except that 2mm thick aluminium was used at the tubehead, instead of PMMA. The grid was removed and an ion chamber was positioned above the detector cover, 40mm from the chest wall edge (CWE). The incident air kerma was measured for a range of manually set mAs values at 34kV Rh/Ag. The readings were corrected to the surface of the detector using the inverse square law. No correction was made for attenuation by the detector cover. A 10mm x 10 mm region of interest (ROI) was positioned on the midline, 40mm from the CWE of each image. The average pixel value and the standard deviation of pixel values within the ROI were measured. The relationship between average pixel values and the air kerma incident at the detector was determined.

## 2.4 Dose measurement

Doses were measured using the AEC in the different modes to expose different thicknesses of PMMA. Each PMMA block had an area of 180mm x 240mm. Spacers were used to adjust the paddle height to be equal to the equivalent breast thickness, as shown in Table 3. The exposure factors were noted and mean glandular doses (MGDs) were calculated for equivalent breast thicknesses. The value of s used in the calculation of MGD for the Rh/Ag target filter combination was 1.087.

An aluminium square, 10mm x 10mm and 0.2mm thick, was used with the PMMA blocks during these exposures, so that the images produced could be used for the calculation of the contrast-to-noise ratio (CNR), described in Section 2.5. The aluminium square was placed between two 10mm thick slabs of 180mm x 240mm PMMA, on the midline, with its centre 60mm from the CWE. Additional layers of PMMA were placed on top to vary the total thickness.

## 2.5 Contrast-to-noise ratio

Unprocessed images acquired during the dose measurement were analysed to obtain the CNRs. Thirty six small square ROIs (approximately 2.5mm x 2.5mm) were used to determine the average signal and the standard deviation in the signal within the image of the aluminium square (4 ROIs) and the surrounding background (32 ROIs), as shown in Figure 2. Small ROIs are used to minimise distortions due to the heel effect and other causes of non-uniformity.[5] The CNR was calculated for each image, as defined in the NHSBSP and European protocols.

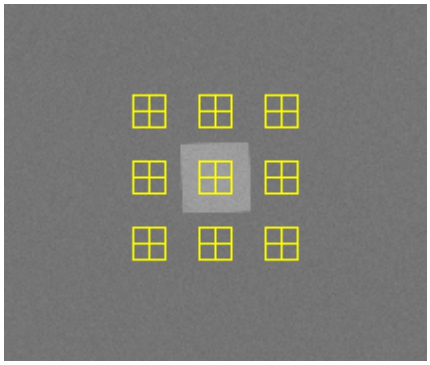

**Figure 2. Location and size of ROI used to determine the CNR**

To apply the standards in the European protocol, it is necessary to relate the image quality measured using the CDMAM (Section 2.8) for an equivalent breast thickness of 60mm, to that for other breast thicknesses. The European protocol[2] gives the relationship between threshold contrast and CNR measurements, enabling the calculation of a target CNR value for a particular level of image quality. This can be compared to CNR measurements made at other breast thicknesses. Contrast for a particular gold thickness is calculated using Equation 1, and target CNR is calculated using Equation 2.

$$\text{Contrast} = 1 - e^{-\mu t} \quad (1)$$

where μ is the effective attenuation coefficient for gold, and t is the gold thickness.

$$\text{CNR}_{\text{target}} = \frac{\text{CNR}_{\text{measured}} \times \text{TC}_{\text{measured}}}{\text{TC}_{\text{target}}} \quad (2)$$

where $\text{CNR}_{\text{measured}}$ is the CNR for a 60mm equivalent breast, $\text{TC}_{\text{measured}}$ is the threshold contrast calculated using the threshold gold thickness for a 0.1mm diameter detail,

(measured using the CDMAM at the same dose as used for $\mathrm{CNR}_{\mathrm{measured}}$), and $\mathrm{TC}_{\mathrm{target}}$ is the calculated threshold contrast corresponding to the threshold gold thickness required to meet either the minimum acceptable or achievable level of image quality as defined in the UK standard.

The threshold gold thickness for the 0.1mm detail diameter is used here because it is generally regarded as the most critical of the detail diameters for which performance standards are set.

The effective attenuation coefficient for gold used in Equation 1 depends on the beam quality used for the exposure, and was selected from a table of values summarised in Table 2. These values were calculated with 3mm PMMA representing the compression paddle, using spectra from Boone et al.[6] and attenuation coefficients for materials in the test objects (aluminium, gold, PMMA) from Berger et al.[7]

The European protocol also defines a limiting value for CNR, which is calculated as a percentage of the threshold contrast for minimum acceptable image quality for each thickness. This limiting value varies with thickness, as shown in Table 3.

**Table 2. Effective attenuation coefficients for gold contrast details in the CDMAM**

| kV | Target/filter | Effective attenuation coefficient ($\mu m^{-1}$) |
|---|---|---|
| 34 | Rh/Ag | 0.110 |

**Table 3. Limiting values for relative CNR**

| Thickness of PMMA (mm) | Equivalent breast thickness (mm) | Limiting values for relative CNR (%) in European protocol |
|---|---|---|
| 20 | 21 | > 115 |
| 30 | 32 | > 110 |
| 40 | 45 | > 105 |
| 45 | 53 | > 103 |
| 50 | 60 | > 100 |
| 60 | 75 | > 95 |
| 70 | 90 | > 90 |

The target CNR values for minimum acceptable and achievable levels of image quality and European limiting values for CNR were calculated. These were compared with the measured CNR results for all breast thicknesses.

## 2.6 AEC performance for local dense areas

This test is described in the supplement to the fourth edition of the European protocol.[3] To simulate local dense areas, images of a 30mm thick block of PMMA of size 180mm x 240mm, were acquired under AEC. Extra PMMA between 2 and 20mm thick and of size 20mm x 40mm was added to provide extra attenuation. The compression plate remained in position at a height of 40mm, as shown in Figure 3. The simulated dense area was positioned 50mm from the CWE of the table.

In the simulated local dense area the mean pixel value and standard deviation for a 10mm x 10mm ROI were measured and the signal-to-noise ratios (SNRs) were calculated.

Measurements were carried out using each of the AEC modes.

Guidance for this test suggests that the SNR for each image should be within 20% of the mean SNR.

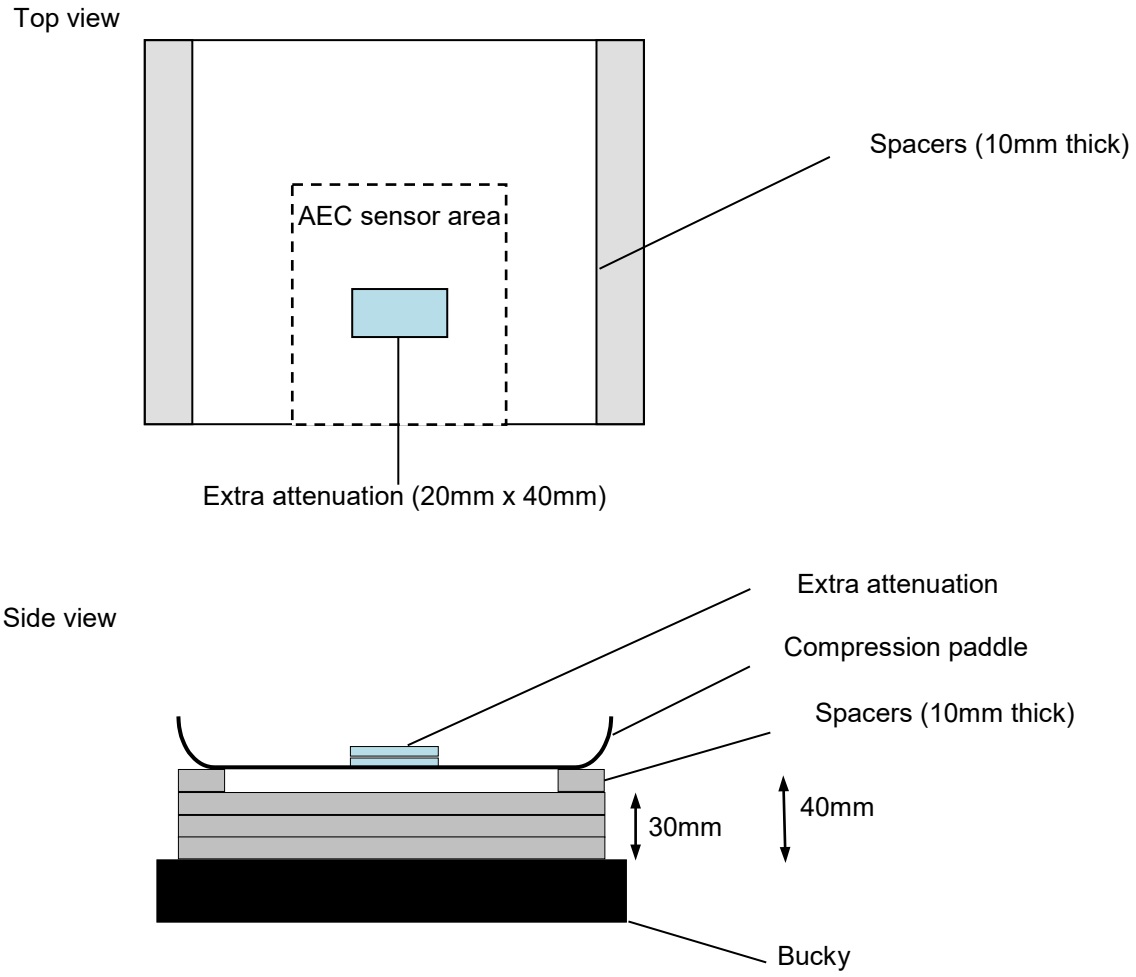


**Figure 3. Setup to measure AEC performance for local dense areas**

## 2.7 Noise analysis

The images acquired in the measurements of detector response, using 34kV Rh/Ag, were used to analyse the image noise. Small ROIs with an area of approximately 2.5mm x 2.5mm were placed on the midline, 60mm from the CWE. The average standard deviations of the pixel values in these ROIs for each image were used to investigate the relationship between the dose to the detector and the image noise. It was assumed that this noise comprises three components: electronic noise, structural noise, and quantum noise. The relationship between them is shown in Equation 3.

$$\sigma_p = \sqrt{k_e^2 + k_q^2 p + k_s^2 p^2} \quad (3)$$

where $\sigma_p$ is the standard deviation in pixel values within an ROI with a uniform exposure and a mean pixel value $p$, and $k_e$, $k_q$, and $k_s$ are the coefficients determining the amount of electronic, quantum, and structural noise in a pixel with a value $p$. This method of analysis has been described previously.[8] For simplicity, the noise is generally presented here as relative noise defined as in Equation 4.

$$\text{Relative noise} = \frac{\sigma_p}{p} \quad (4)$$

The variation in relative noise with mean pixel value was evaluated and fitted using Equation 3, and non-linear regression used to determine the best fit for the constants and their asymptotic confidence limits (using Graphpad Prism version 6.05 for Windows, Graphpad software, San Diego, California, USA, www.graphpad.com). This established whether the experimental measurements of the noise fitted this equation, and the relative proportions of the different noise components. The relationship between noise and pixel values has been found empirically to be approximated by a simple power relationship as shown in Equation 5.

$$\frac{\sigma_p}{p} = k_t p^{-n} \quad (5)$$

where $k_t$ is a constant. If the noise were purely quantum noise the value of $n$ would be 0.5. However the presence of electronic and structural noise means that $n$ can be slightly higher or lower than 0.5.

The variance in pixel values within a ROI is defined as the standard deviation squared. The total variance was plotted against incident air kerma at the detector and fitted using Equation 3. Non-linear regression was used to determine the best fit for the constants and their asymptotic confidence limits, using the Graphpad Prism software.

Using the calculated constants, the structural, electronic, and quantum components of the variance were estimated, assuming that each component was independently related

to incident air kerma. The percentage of the total variance represented by each component was then calculated and plotted against incident air kerma at the detector.

## 2.8 Image quality measurements

Contrast detail measurements were made using a CDMAM phantom (serial number 1022, version 3.4, UMC St. Radboud, Nijmegen University, Netherlands). The phantom was positioned with a 20mm thickness of PMMA above and below, to give a total attenuation approximately equivalent to 50mm of PMMA or 60mm thickness of typical breast tissue. The exposure factors were chosen to be close to those selected by the AEC, in Standard mode, when imaging a 50mm thickness of PMMA. This procedure was repeated to obtain a representative sample of 16 images at this dose level. Further sets of 16 images of the test phantom were then obtained at other dose levels by manually selecting higher and lower mAs values with the same beam quality.

The CDMAM images were read and analysed automatically using Version 1.6 of CDCOM[9,10] and Version 2.1.0 of CDMAM Analysis (available on request from www.nccpm.org). The threshold gold thickness for a typical human observer was predicted using Equation 6.

$$\mathrm{TC}_{\mathrm{predicted}} = \mathrm{r}\mathrm{TC}_{\mathrm{auto}} \qquad (6)$$

where $\mathrm{TC}_{\mathrm{predicted}}$ is the predicted threshold contrast for a typical observer, $\mathrm{TC}_{\mathrm{auto}}$ is the threshold contrast measured using an automated procedure with CDMAM images. $\mathrm{r}$ is the average ratio between human and automatic threshold contrast determined experimentally with the values shown in Table 4.

**Table 4. Values of r used to predict threshold contrast**

| Diameter of gold disc (mm) | Average ratio of human to automatically measured threshold contrast (r) |
|---|---|
| 0.08 | 1.40 |
| 0.10 | 1.50 |
| 0.13 | 1.60 |
| 0.16 | 1.68 |
| 0.20 | 1.75 |
| 0.25 | 1.82 |
| 0.31 | 1.88 |
| 0.40 | 1.94 |
| 0.50 | 1.98 |
| 0.63 | 2.01 |
| 0.80 | 2.06 |
| 1.00 | 2.11 |

The predicted threshold gold thickness for each detail diameter in the range 0.1mm to 1.0mm was fitted with a curve for each dose level, using the relationship shown in Equation 7.

$$\text{Threshold gold thickness} = a + bx^{-1} + cx^{-2} + dx^{-3} \quad (7)$$

where $x$ is the detail diameter, and $a$, $b$, $c$ and $d$ are coefficients adjusted to obtain a least squares fit.

The confidence limits for the predicted threshold gold thicknesses have been previously determined by a sampling method using a large set of images. The threshold contrasts quoted in the tables of results are derived from the fitted curves, as this has been found to improve accuracy.

The expected relationship between threshold contrast and dose is shown in Equation 8.

$$\text{Threshold contrast} = \lambda D^{-n} \quad (8)$$

where $D$ is the MGD for a 60mm thick standard breast (equivalent to the test phantom configuration used for the image quality measurement), and $\lambda$ is a constant to be fitted.

It is assumed that a similar equation applies when using threshold gold thickness instead of contrast. This equation was plotted with the experimental data for detail diameters of 0.1 and 0.25mm. The value of $n$ resulting in the best fit to the experimental data was determined, and the doses required for target CNR values were calculated for data relating to these detail diameters.

## 2.9 Physical measurements of the detector performance

The presampled modulation transfer function (MTF), normalised noise power spectrum (NNPS) and the detective quantum efficiency (DQE) of the system were measured. The methods used were as close as possible to those described by the International Electrotechnical Commission (IEC).[11] The radiation quality used for the measurements was adjusted by placing a uniform 2mm thick aluminium filter at the tube housing. The beam quality used was 26kV Mo/Mo. The test device to measure the MTF comprised a 120mm x 60mm rectangle of stainless steel with polished straight edges, of thickness 0.8mm. The grid was removed by sliding the complete bucky out and then the MTF test device was placed on the detector entrance cover. The test device was positioned to measure the MTF in two directions, first almost perpendicular to the CWE and then almost parallel to it. A 10th order polynomial fit was applied to the results.

To measure the noise power spectrum the test device was removed and exposures made for a range of incident air kerma at the surface of the table. The DQE is presented

as the average of measurements in the directions perpendicular and parallel to the CWE.

### 2.10 Other tests

Other tests were carried out to cover the range that would normally form part of a commissioning survey on new equipment. These included tests prescribed in IPEM Report 89[4] for mammographic X-ray sets, as well as those in the UK NHSBSP protocol for digital mammographic systems

# 3. Results

## 3.1 Output and HVL

The output and HVL measurements are shown in Table 5.

**Table 5. Output and HVL**

| kV | Target/filter | Output (μGy/mAs at 1m) | HVL (mm Al) | Focus |
|---|---|---|---|---|
| 26 | Mo/Mo | 26.7 | 0.344 | Large |
| 29 | Mo/Mo | 38.3 | 0.375 | Small |
| 34 | Rh/Ag | 45.2 | 0.539 | Large |

The tube voltage measurements are shown in Table 6. All were within 0.3kV of indicated values and are within the IPEM Report 89[4] remedial level of ±1kV.

**Table 6. kV measurements made with Mo/Mo target/filter combination**

| kV set | kV measured |
|---|---|
| 26 | 25.8 |
| 28 | 27.9 |
| 30 | 30.2 |
| 32 | 32.3 |

## 3.2 Detector response

The detector response is shown in Figure 4.

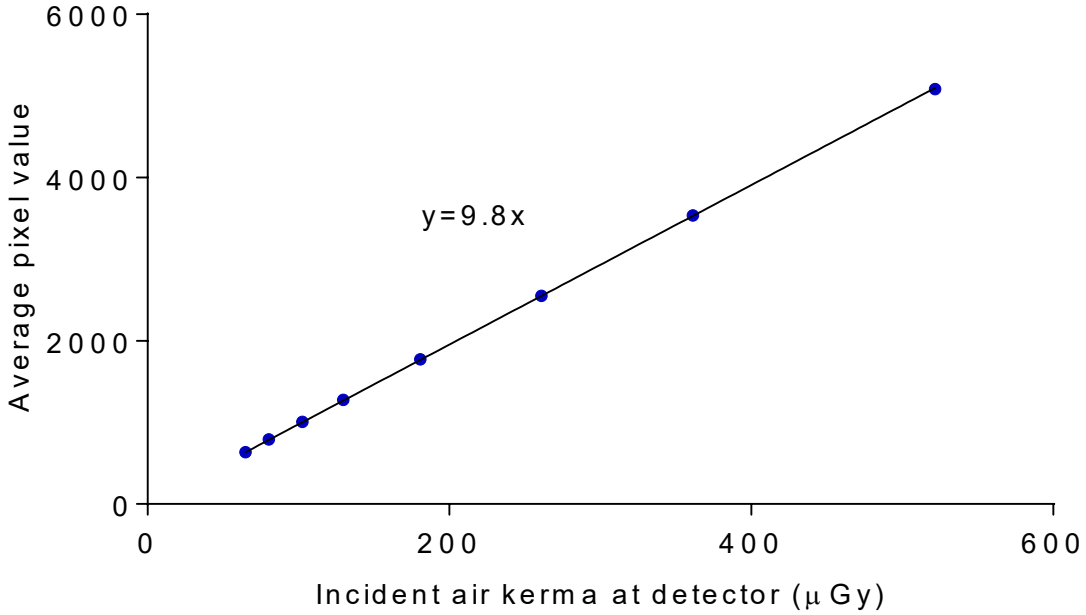


**Figure 4. Detector response acquired at 34kV Rh/Ag anode/filter combination with 2mm Al at the tube port**

## 3.3 AEC performance

### 3.3.1 Dose

The MGDs for breasts simulated with PMMA, exposed using the 4 different AEC modes, are shown in Figure 5 and Tables 7 to 10. The MGDs include the pre-pulse exposure, which is not included in the stated mAs values.

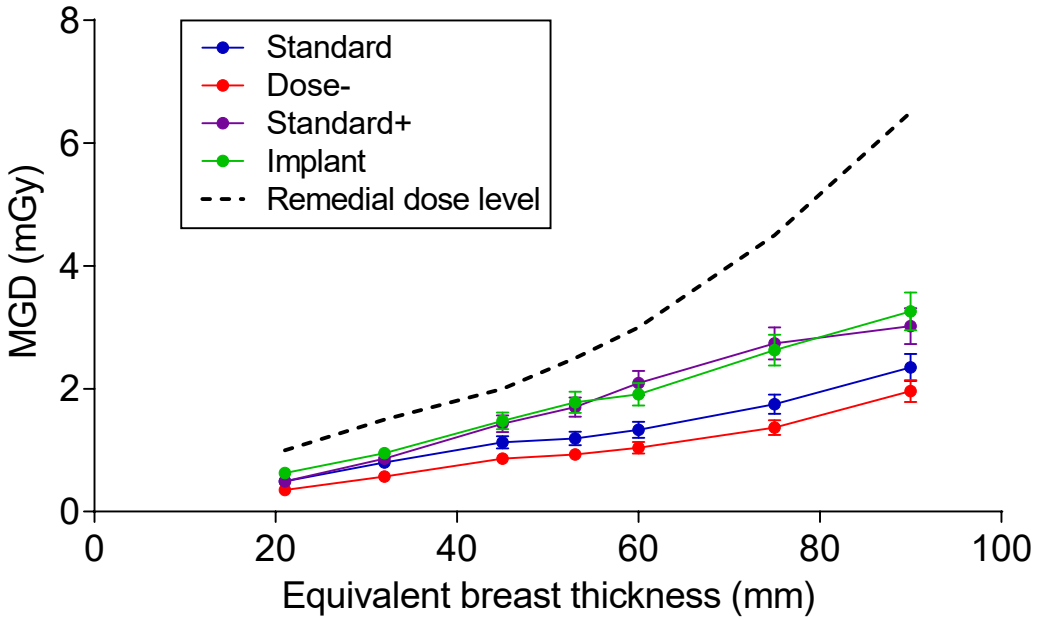


**Figure 5 MGD for different thicknesses of simulated breasts in the 4 AEC modes. (Error bars indicate 95% confidence limits.)**

**Table 7. MGD for simulated breasts, AEC Standard mode**

| PMMA thick-ness (mm) | Equivalent breast thickness (mm) | kV | Target/ filter | mAs | MGD (mGy) | Remedial dose level (mGy) | Displ-ayed dose (mGy) | Displayed % higher than measured |
|---|---|---|---|---|---|---|---|---|
| 20 | 21 | 26 | Mo/Mo | 16.9 | 0.49 | 1.0 | 0.51 | 5 |
| 30 | 32 | 26 | Mo/Mo | 38.8 | 0.80 | 1.5 | 0.84 | 5 |
| 40 | 45 | 34 | Rh/Ag | 23.8 | 1.13 | 2.0 | 1.16 | 3 |
| 45 | 53 | 34 | Rh/Ag | 27.7 | 1.19 | 2.5 | 1.25 | 5 |
| 50 | 60 | 34 | Rh/Ag | 33.4 | 1.33 | 3.0 | 1.39 | 4 |
| 60 | 75 | 34 | Rh/Ag | 48.6 | 1.75 | 4.5 | 1.85 | 6 |
| 70 | 90 | 34 | Rh/Ag | 77.2 | 2.35 | 6.5 | 2.55 | 8 |

**Table 8. MGD for simulated breasts, AEC Dose- mode**

| PMMA thick-ness (mm) | Equivalent breast thickness (mm) | kV | Target/ filter | mAs | MGD (mGy) | Remedial dose level (mGy) | Displ-ayed dose (mGy) | Displayed % higher than measured |
|---|---|---|---|---|---|---|---|---|
| 20 | 21 | 26 | Mo/Mo | 11.8 | 0.35 | 1.0 | 0.37 | 4 |
| 30 | 32 | 26 | Mo/Mo | 27.3 | 0.57 | 1.5 | 0.60 | 5 |
| 40 | 45 | 34 | Rh/Ag | 17.8 | 0.86 | 2.0 | 0.89 | 3 |
| 45 | 53 | 34 | Rh/Ag | 21.1 | 0.93 | 2.5 | 0.97 | 5 |
| 50 | 60 | 34 | Rh/Ag | 25.5 | 1.04 | 3.0 | 1.07 | 3 |
| 60 | 75 | 34 | Rh/Ag | 37.2 | 1.37 | 4.5 | 1.44 | 5 |
| 70 | 90 | 34 | Rh/Ag | 63.5 | 1.96 | 6.5 | 2.12 | 8 |

**Table 9. MGD for simulated breasts, AEC Standard+ mode**

| PMMA thick-ness (mm) | Equivalent breast thickness (mm) | kV | Target/ filter | mAs | MGD (mGy) | Remedial dose level (mGy) | Displ-ayed dose (mGy) | Displayed % higher than measured |
|---|---|---|---|---|---|---|---|---|
| 20 | 21 | 26 | Mo/Mo | 16.9 | 0.49 | 1.0 | 0.51 | 5 |
| 30 | 32 | 26 | Mo/Mo | 42.1 | 0.86 | 1.5 | 0.90 | 4 |
| 40 | 45 | 34 | Rh/Ag | 30.8 | 1.43 | 2.0 | 1.45 | 1 |
| 45 | 53 | 34 | Rh/Ag | 40.3 | 1.70 | 2.5 | 1.78 | 5 |
| 50 | 60 | 34 | Rh/Ag | 53.5 | 2.09 | 3.0 | 2.17 | 4 |
| 60 | 75 | 34 | Rh/Ag | 78.5 | 2.74 | 4.5 | 2.90 | 6 |
| 70 | 90 | 34 | Rh/Ag | 100.3 | 3.02 | 6.5 | 3.27 | 8 |

**Table 10. MGD for simulated breasts, AEC Implant mode**

| PMMA thick-ness (mm) | Equivalent breast thickness (mm) | kV | Target/ filter | mAs | MGD (mGy) | Remedial dose level (mGy) | Displ-ayed dose (mGy) | Displayed % higher than measured |
|---|---|---|---|---|---|---|---|---|
| 20 | 21 | 26 | Mo/Mo | 22.7 | 0.58 | 1.0 | 0.63 | -12 |
| 30 | 32 | 26 | Mo/Mo | 46.7 | 0.91 | 1.5 | 0.95 | 1 |
| 40 | 45 | 34 | Rh/Ag | 31.8 | 1.39 | 2.0 | 1.48 | -2 |
| 45 | 53 | 34 | Rh/Ag | 42.5 | 1.70 | 2.5 | 1.78 | -1 |
| 50 | 60 | 34 | Rh/Ag | 48.8 | 1.84 | 3.0 | 1.91 | -1 |
| 60 | 75 | 34 | Rh/Ag | 75.2 | 2.50 | 4.5 | 2.63 | -1 |
| 70 | 90 | 34 | Rh/Ag | 108.3 | 3.14 | 6.5 | 3.26 | 2 |

### 3.3.2 Contrast-to-noise ratio

The results of the CNR measurements are shown in Figure 6 and Tables 11 to 12. The following calculated values are also shown:

- CNR to meet the minimum acceptable image quality (IQ) standard at the 60mm breast thickness
- CNR to meet the achievable image quality standard at the 60mm breast thickness
- CNRs at each thickness to meet the limiting value in the European protocol

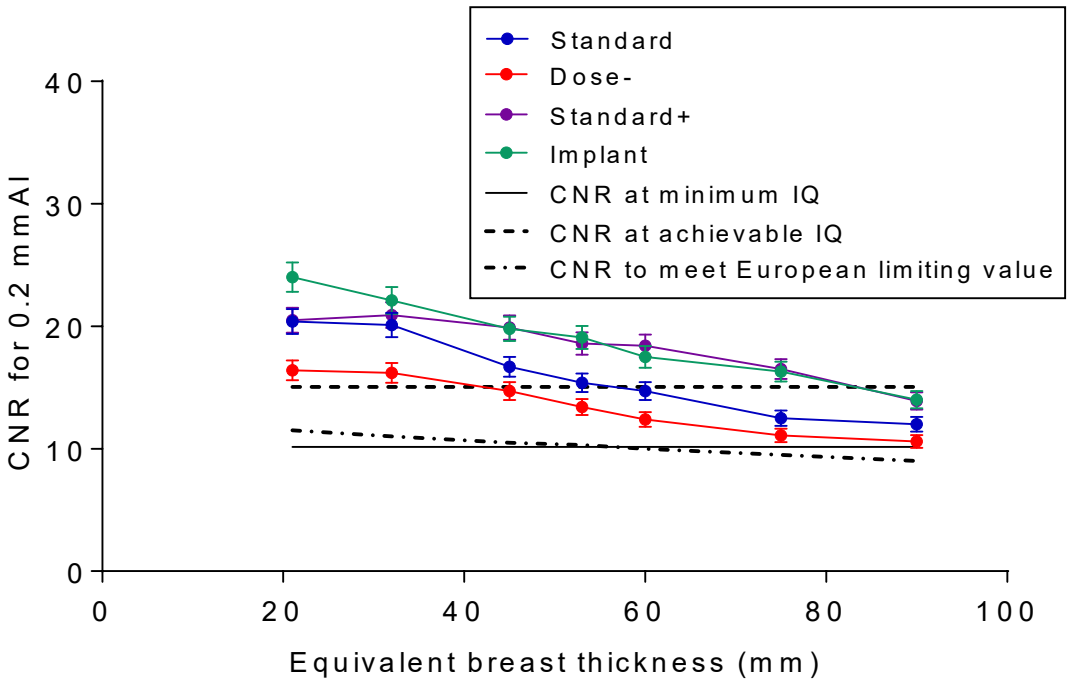


**Figure 6. CNR measured at the 4 AEC modes. (Error bars indicate 95% confidence limits.)**

**Table 11. CNR measurements, AEC Standard mode**

| PMMA thickness (mm) | Equivalent breast thick-ness (mm) | Measured CNR | CNR for minimum acceptable IQ | CNR for achievable IQ | European limiting CNR value |
|---|---|---|---|---|---|
| 20 | 21 | 20.4 | 10.0 | 14.9 | 11.5 |
| 30 | 32 | 20.1 | 10.0 | 14.9 | 11.0 |
| 40 | 45 | 16.7 | 10.0 | 14.9 | 10.5 |
| 45 | 53 | 15.4 | 10.0 | 14.9 | 10.3 |
| 50 | 60 | 14.7 | 10.0 | 14.9 | 10.0 |
| 60 | 75 | 12.5 | 10.0 | 14.9 | 9.5 |
| 70 | 90 | 12.0 | 10.0 | 14.9 | 9.0 |

**Table 12. CNR measurements, AEC dose modes compared**

| PMMA thickness (mm) | Equivalent breast thick-ness (mm) | Measured CNR Standard | Measured CNR Dose- | Measured CNR Standard+ | Measured CNR Implant |
|---|---|---|---|---|---|
| 20 | 21 | 20.4 | 16.4 | 20.5 | 24.0 |
| 30 | 32 | 20.1 | 16.2 | 20.9 | 22.1 |
| 40 | 45 | 16.7 | 14.7 | 19.9 | 19.8 |
| 45 | 53 | 15.4 | 13.4 | 18.6 | 19.1 |
| 50 | 60 | 14.7 | 12.4 | 18.4 | 17.5 |
| 60 | 75 | 12.5 | 11.1 | 16.5 | 16.3 |
| 70 | 90 | 12.0 | 10.6 | 13.9 | 14.0 |

### 3.3.3 AEC performance for local dense areas

For many systems, when the AEC adjusts for locally dense areas, the SNR remains constant with increasing thickness of extra PMMA. The results of this test are shown in Tables 13 to16 and Figure 7. The need for a more suitable test for the Pristina, for which the aim is to keep CNR (rather than SNR) constant, is discussed in section 4.

For Standard, Dose- and Standard+ modes, the first 2 exposures are at 26kV Mo/Mo. For greater thicknesses the exposures are at 34kV Rh/Ag and the SNR jumps to a higher value, and then decreases only slowly with increasing thickness of PMMA. In Implant mode, all exposures are at 34kV Rh/Ag, and the SNR decreases slowly from the initial value.

Most SNR values are within the suggested limit of 20% of the mean SNR. Only for the Mo/Mo exposures. The implant mode is designed to give exposures dependent on the breast thickness, therefore this test is not relevant.

**Table 13. AEC performance for local dense areas, AEC Standard mode**

| Total attenuation (mm PMMA) | kV | Target/ filter | Tube load (mAs) | SNR | % difference from average |
|---|---|---|---|---|---|
| 32 | 26 | Mo/Mo | 45.7 | 98.1 | -20 |
| 34 | 26 | Mo/Mo | 54.2 | 97.1 | -21 |
| 36 | 34 | Rh/Ag | 20.7 | 140.8 | 15 |
| 38 | 34 | Rh/Ag | 22.2 | 139.1 | 14 |
| 40 | 34 | Rh/Ag | 23.7 | 135.2 | 10 |
| 42 | 34 | Rh/Ag | 24.7 | 128.3 | 5 |
| 44 | 34 | Rh/Ag | 26.6 | 126.5 | 3 |
| 46 | 34 | Rh/Ag | 27.6 | 123.1 | 0 |
| 48 | 34 | Rh/Ag | 30.0 | 120.0 | -2 |
| 50 | 34 | Rh/Ag | 31.8 | 117.2 | -4 |

**Table 14. AEC performance for local dense areas, AEC Dose- mode**

| Total attenuation (mm PMMA) | kV | Target/ filter | Tube load (mAs) | SNR | % difference from average |
|---|---|---|---|---|---|
| 32 | 26 | Mo/Mo | 32.0 | 79.4 | -24 |
| 34 | 26 | Mo/Mo | 37.7 | 80.3 | -23 |
| 36 | 34 | Rh/Ag | 15.0 | 117.6 | 13 |
| 38 | 34 | Rh/Ag | 16.0 | 114.9 | 10 |
| 40 | 34 | Rh/Ag | 17.6 | 114.4 | 10 |
| 42 | 34 | Rh/Ag | 18.6 | 111.4 | 7 |
| 44 | 34 | Rh/Ag | 20.3 | 111.4 | 7 |
| 46 | 34 | Rh/Ag | 21.2 | 106.6 | 2 |
| 48 | 34 | Rh/Ag | 23.0 | 102.3 | -2 |

**Table 15. AEC performance for local dense areas, AEC Standard+ mode**

| Total attenuation (mm PMMA) | kV | Target/ filter | Tube load (mAs) | SNR | % difference from average |
|---|---|---|---|---|---|
| 32 | 26 | Mo/Mo | 49.6 | 102.0 | -27 |
| 34 | 26 | Mo/Mo | 59.9 | 101.8 | -27 |
| 36 | 34 | Rh/Ag | 24.4 | 152.5 | 9 |
| 38 | 34 | Rh/Ag | 26.5 | 153.7 | 10 |
| 40 | 34 | Rh/Ag | 30.1 | 149.1 | 7 |
| 42 | 34 | Rh/Ag | 32.8 | 150.1 | 7 |
| 44 | 34 | Rh/Ag | 37.0 | 149.2 | 7 |
| 46 | 34 | Rh/Ag | 40.1 | 148.3 | 6 |
| 48 | 34 | Rh/Ag | 45.4 | 143.5 | 3 |
| 50 | 34 | Rh/Ag | 49.4 | 149.6 | 7 |

**Table 16. AEC performance for local dense areas, AEC Implant mode**

| Total attenuation (mm PMMA) | kV | Target/ filter | Tube load (mAs) | SNR | % difference from average |
|---|---|---|---|---|---|
| 32 | 34 | Rh/Ag | 25.2 | 174.8 | 27 |
| 34 | 34 | Rh/Ag | 26.5 | 169.4 | 23 |
| 36 | 34 | Rh/Ag | 26.5 | 158.6 | 15 |
| 38 | 34 | Rh/Ag | 25.2 | 147.6 | 7 |
| 40 | 34 | Rh/Ag | 25.2 | 136.0 | -1 |
| 42 | 34 | Rh/Ag | 26.5 | 134.3 | -2 |
| 44 | 34 | Rh/Ag | 25.2 | 120.8 | -12 |
| 46 | 34 | Rh/Ag | 26.5 | 120.1 | -13 |
| 48 | 34 | Rh/Ag | 25.2 | 109.9 | -20 |
| 50 | 34 | Rh/Ag | 25.2 | 103.5 | -25 |

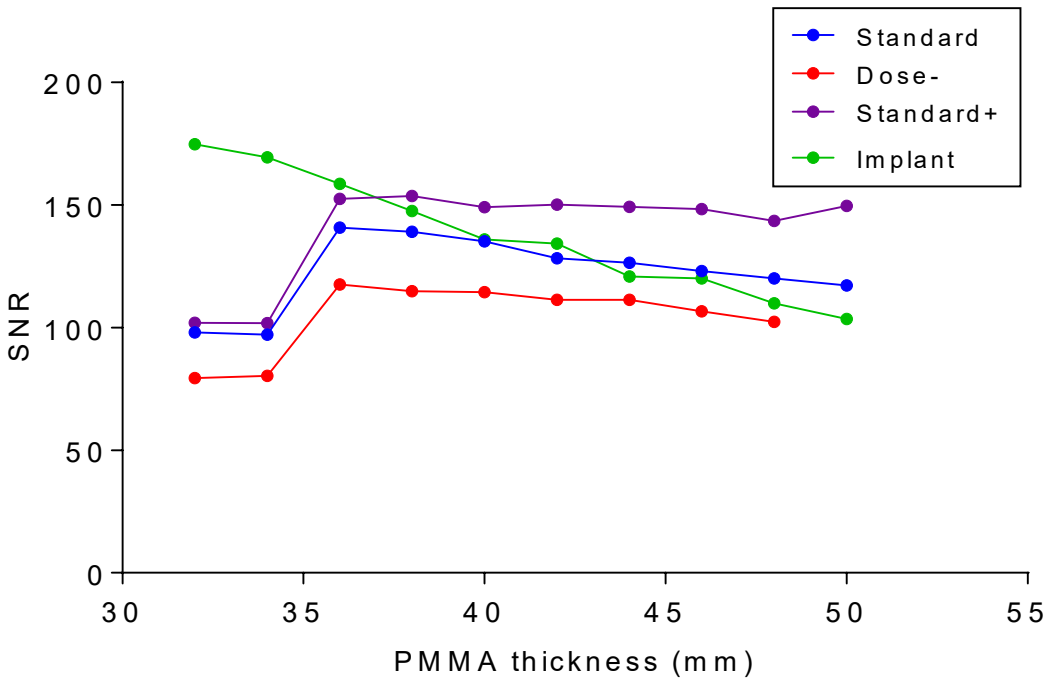


**Figure 7. AEC performance (4 modes) in local dense area test**

## 3.4 Noise measurements

The variation in noise with dose was analysed by plotting the standard deviation in pixel values against the incident air kerma at the detector, as shown in Figure 8. The fitted

power curve has an index of 0.54, which is close to the expected value of 0.5 for quantum noise sources alone.

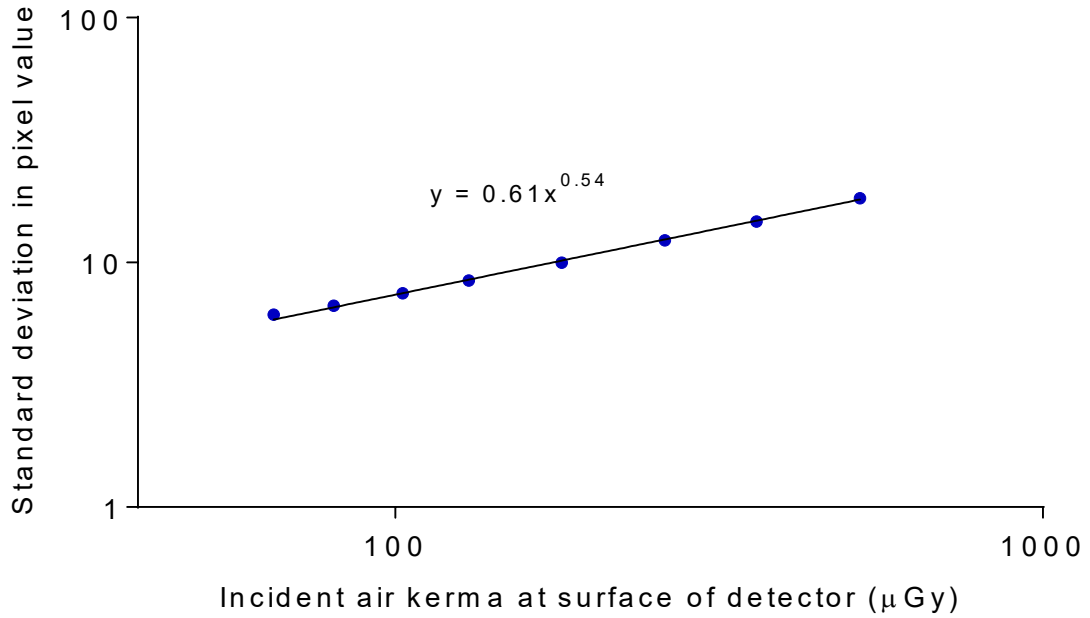


**Figure 8. Standard deviation of pixel values versus incident air kerma at detector**

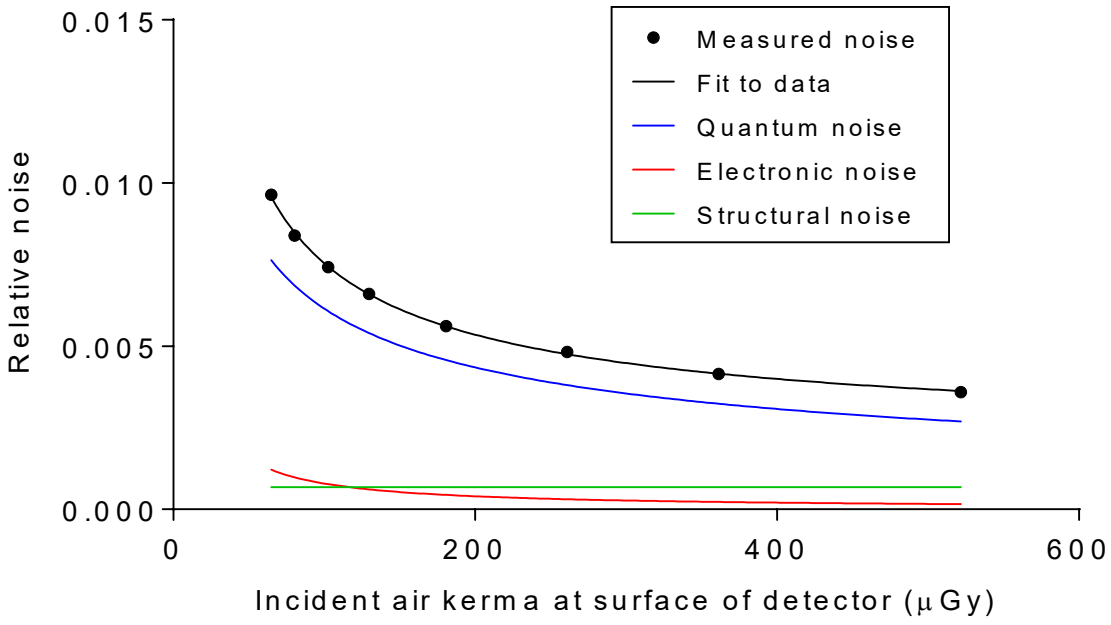


**Figure 9. Relative noise and noise components**

Figure 9 shows the relative noise at different incident air kerma. The estimated relative contributions of electronic, structural, and quantum noise are shown and the quadratic sum of these contributions fitted to the measured noise (using Equation 3).

Figure 10 shows the different amounts of variance due to each component; the quantum variance is seen to predominate.

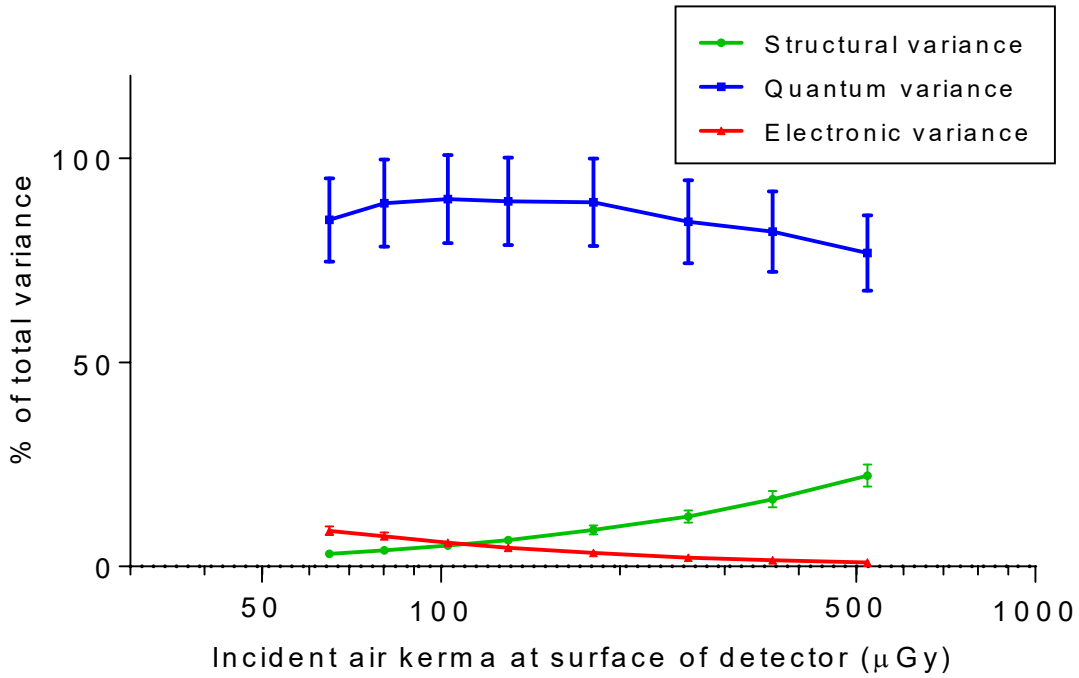


**Figure 10. Noise components as a percentage of the total variance. (Error bars indicate 95% confidence limits.)**

## 3.5 Image quality measurements

The exposure factors used for each set of 16 CDMAM images are shown in Table 17.

**Table 17. Images acquired for image quality measurement**

| kV | Target/filter | Tube load (mAs) | Mean glandular dose to equivalent breasts 60mm thick (mGy) |
|---|---|---|---|
| 34 | Rh/Ag | 16 | 0.60 |
| 34 | Rh/Ag | 22 | 0.83 |
| 34 | Rh/Ag | 32 | 1.21 |
| 34 | Rh/Ag | 45 | 1.70 |
| 34 | Rh/Ag | 63 | 2.37 |

The contrast detail curves (determined by automatic reading of the images) at the different dose levels are shown in Figure 11. The threshold gold thicknesses measured for different detail diameters at the 5 selected dose levels are shown in Table 18. The NHSBSP minimum acceptable and achievable limits are also shown.

The measured threshold gold thicknesses are plotted against the MGD for an equivalent breast for the 0.1mm and 0.25mm detail sizes in Figure 12.

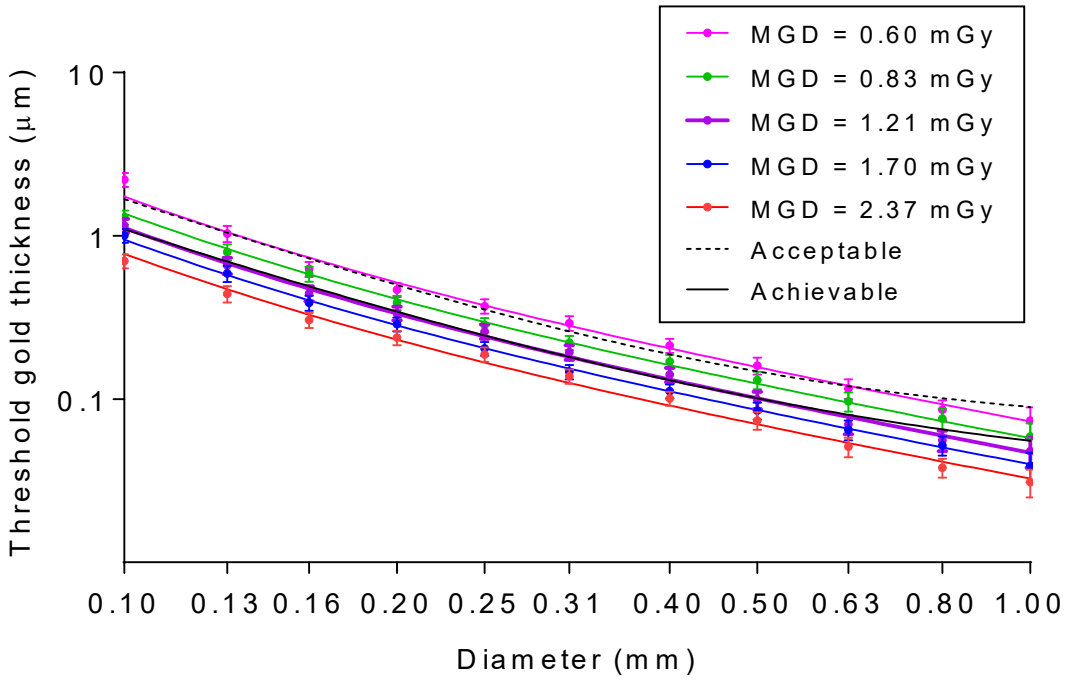


**Figure 11. Contrast-detail curves for 5 doses at 34kV Rh/Ag. (Error bars indicate 95% confidence limits.)**

**Table 18. Average threshold gold thicknesses for different detail diameters for 5 doses using 34kV Rh/Ag, and automatically predicted data**

| Diam-eter (mm) | Threshold gold thickness (µm) | | | | | | |
|---|---|---|---|---|---|---|---|
| | Accept-able value | Achiev-able value | MGD = 0.60mGy | MGD = 0.83mGy | MGD = 1.21mGy | MGD = 1.70mGy | MGD = 2.37mGy |
| 0.1 | 1.680 | 1.100 | 2.21 ± 0.22 | 1.30 ± 0.13 | 1.16 ± 0.11 | 1.00 ± 0.01 | 0.70 ± 0.07 |
| 0.25 | 0.352 | 0.244 | 0.371± 0.037 | 0.285 ± 0.029 | 0.260± 0.026 | 0.204 ± 0.020 | 0.188 ± 0.019 |
| 0.5 | 0.150 | 0.103 | 0.160 ± 0.019 | 0.31± 0.02 | 0.099 ± 0.012 | 0.085 ± 0.010 | 0.074 ± 0.009 |
| 1.0 | 0.091 | 0.056 | 0.074 ± 0.015 | 0.059± 0.012 | 0.048 ± 0.010 | 0.039 ± 0.008 | 0.031 ± 0.006 |

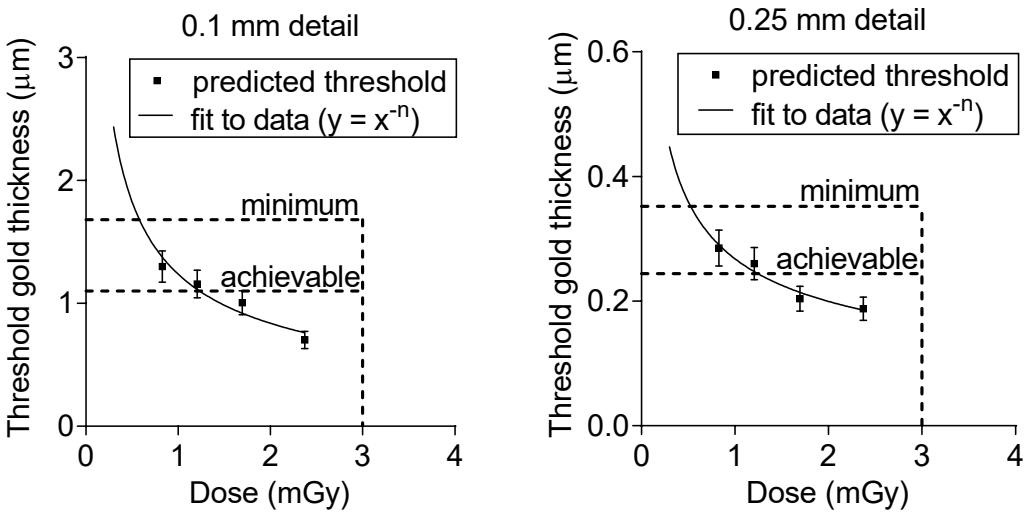


**Figure 12. Threshold gold thickness at different doses. (Error bars indicate 95% confidence limits.)**

## 3.6 Comparison with other systems

The MGDs to reach the minimum and achievable image quality standards in the NHSBSP protocol have been estimated from the curves shown in Figure 12. The fitted curves are of the form $y = x^{-n}$. (The error in estimating these doses depends on the accuracy of the curve fitting procedure, and pooled data for several systems has been used to estimate the 95% confidence limits of about 20%.) These doses are shown against similar data for different models of digital mammography systems in Tables 19 and 20 and Figures 13 to 16. The data for these systems has been determined in the same way as described in this report and the results published previously.[12-18] The data for film-screen represents an average value determined using a variety of film-screen systems in use prior to their discontinuation.

**Table 19. The MGD for a 60mm equivalent breast for different systems to reach the minimum acceptable threshold gold thickness for 0.1mm and 0.25mm details**

| System | MGD (mGy) for 0.1mm | MGD (mGy) for 0.25mm |
|---|---|---|
| **GE Pristina** | **0.58 ± 0.12** | **0.53 ± 0.10** |
| GE Essential | 0.49 ± 0.10 | 0.49 ± 0.10 |
| Fujifilm Innovality | 0.61 ± 0.12 | 0.49 ± 0.10 |
| Giotto Class | 0.50 ± 0.10 | 0.40 ± 0.08 |
| Hologic 3Dimensions | 0.40 ± 0.08 | 0.33 ± 0.07 |
| Philips MicroDose L30 C120 | 0.67 ± 0.13 | 0.47 ± 0.09 |
| Planmed Clarity | 0.60 ± 0.12 | 0.49 ± 0.10 |
| Siemens Revelation | 0.43 ± 0.09 | 0.39 ± 0.08 |
| Film-screen | 1.30 ± 0.26 | 1.36 ± 0.27 |

**Table 20. The MGD for a 60mm equivalent breast for different systems to reach the achievable threshold gold thickness for 0.1mm and 0.25mm details**

| System | MGD (mGy) for 0.1mm | MGD (mGy) for 0.25mm |
|---|---|---|
| **GE Pristina** | **1.23 ± 0.25** | **1.25 ± 0.25** |
| GE Essential | 1.13 ± 0.23 | 1.03 ± 0.21 |
| Fujifilm Innovality | 1.15 ± 0.23 | 1.02 ± 0.20 |
| Giotto Class | 1.06 ± 0.21 | 1.05 ± 0.21 |
| Hologic 3Dimensions | 0.78 ± 0.16 | 0.74 ± 0.15 |
| Philips MicroDose L30 C120 | 1.34 ± 0.27 | 1.06 ± 0.21 |
| Planmed Clarity | 1.15 ± 0.23 | 1.02 ± 0.20 |
| Siemens Revelation | 0.82 ± 0.17 | 0.85 ± 0.17 |
| Film-screen | 3.03 ± 0.61 | 2.83 ± 0.57 |

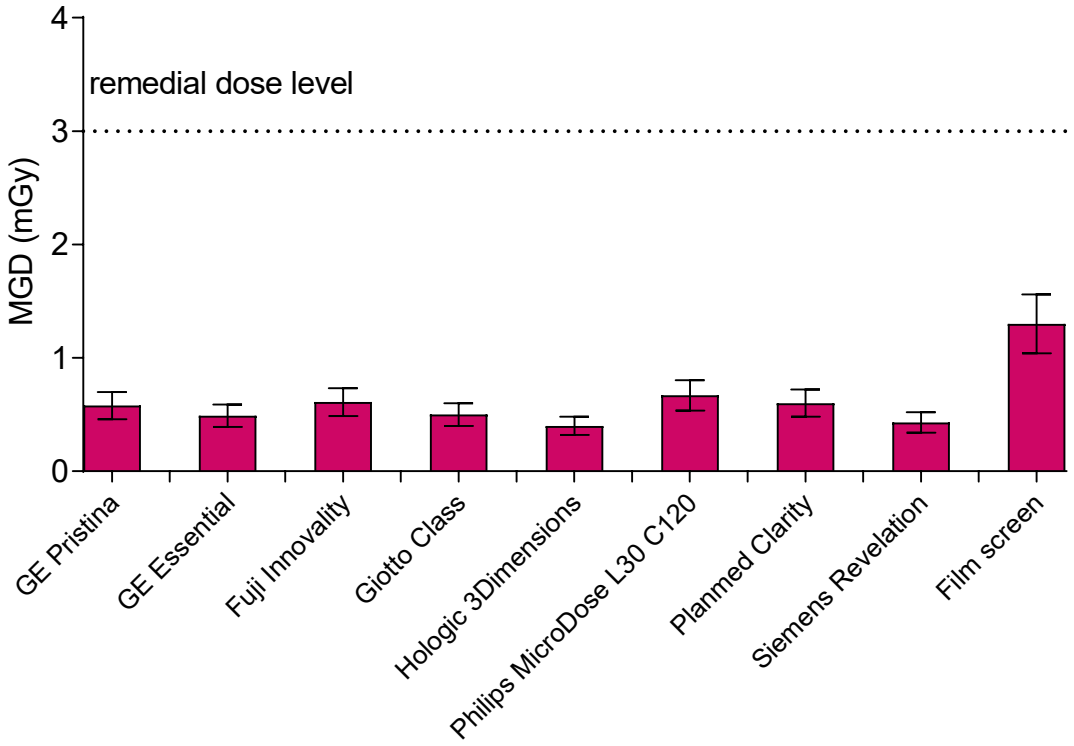


**Figure 13. MGD for a 60mm equivalent breast to reach minimum acceptable image quality standard for 0.1mm detail. (Error bars indicate 95% confidence limits.)**

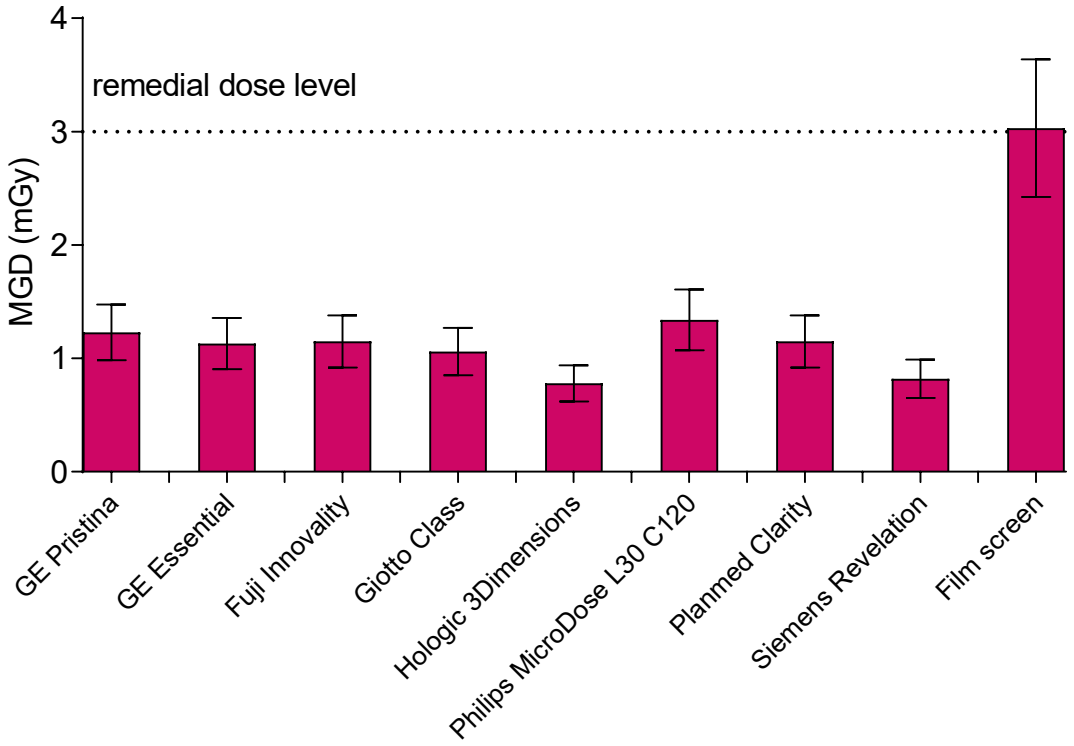


**Figure 14. MGD for a 60mm equivalent breast to reach achievable image quality standard for 0.1mm detail. (Error bars indicate 95% confidence limits.)**

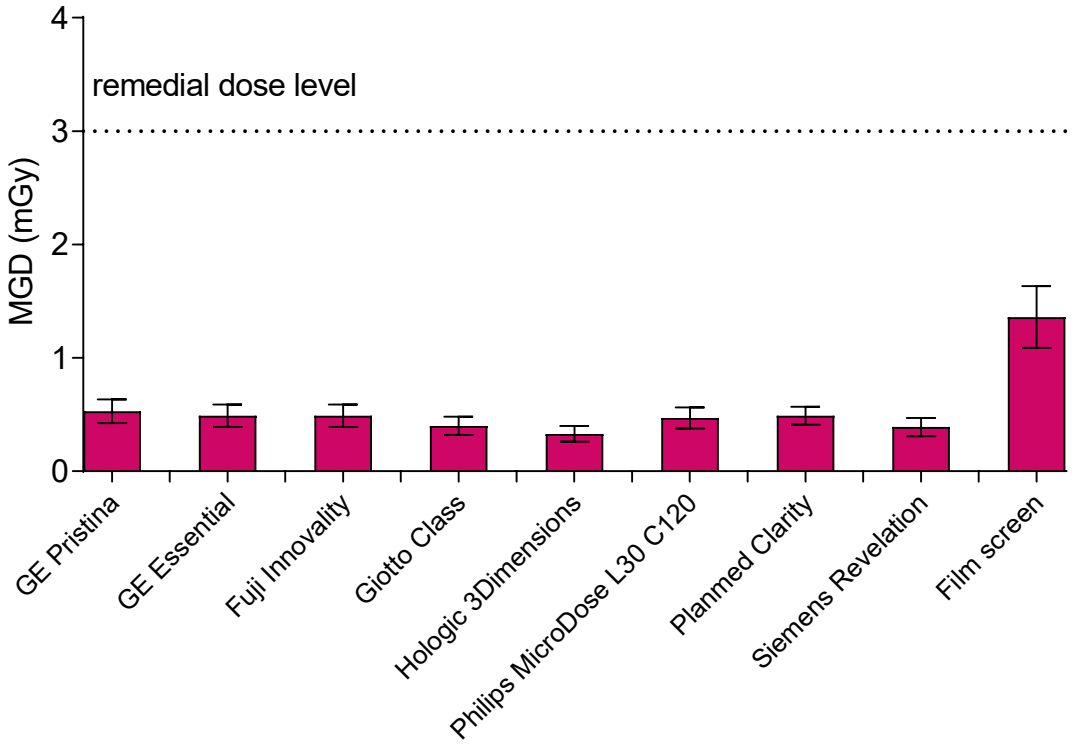


**Figure 15. MGD for a 60mm equivalent breast to reach minimum acceptable image quality standard for 0.25mm detail. (Error bars indicate 95% confidence limits.)**

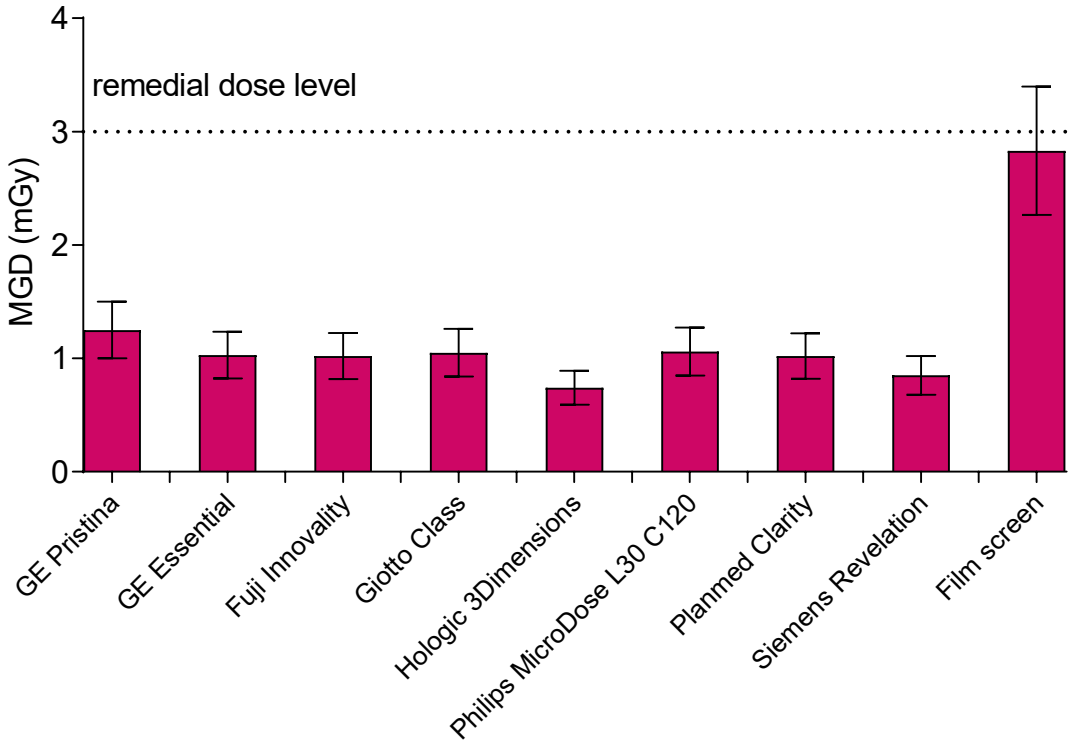


**Figure 16. MGD for a 60mm equivalent breast to reach achievable image quality standard for 0.25mm detail. (Error bars indicate 95% confidence limits.)**

## 3.7 Detector performance

The MTF is shown in Figure 17 for the two orthogonal directions. Figure 18 shows the NNPS curves for a range of air kerma incident to the detector.

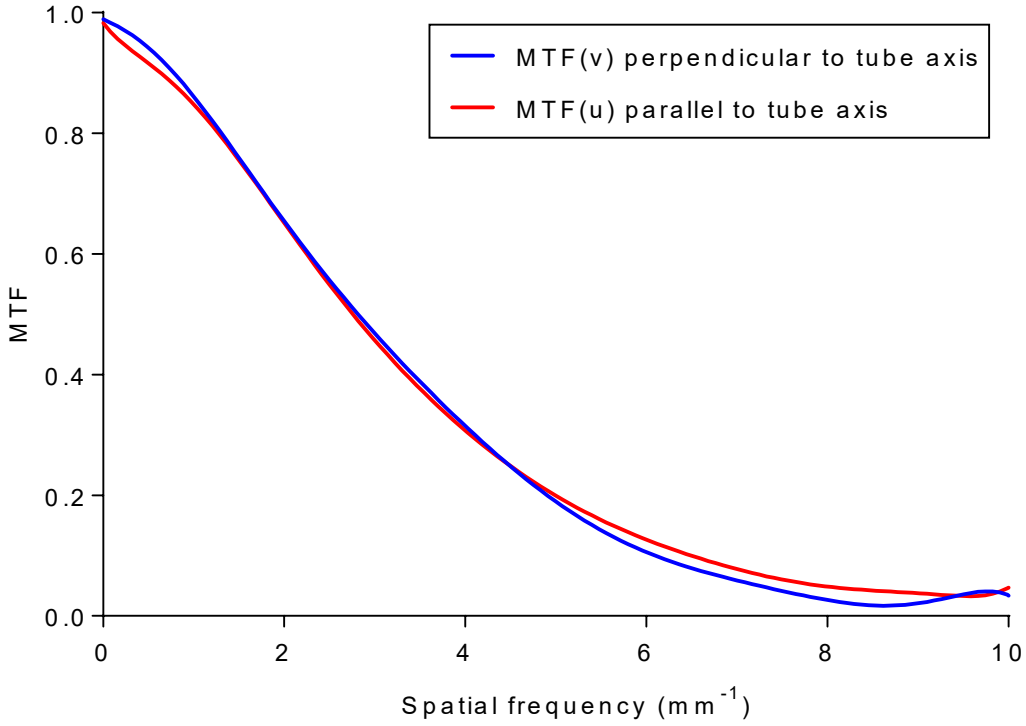


**Figure 17. Pre-sampling MTF**

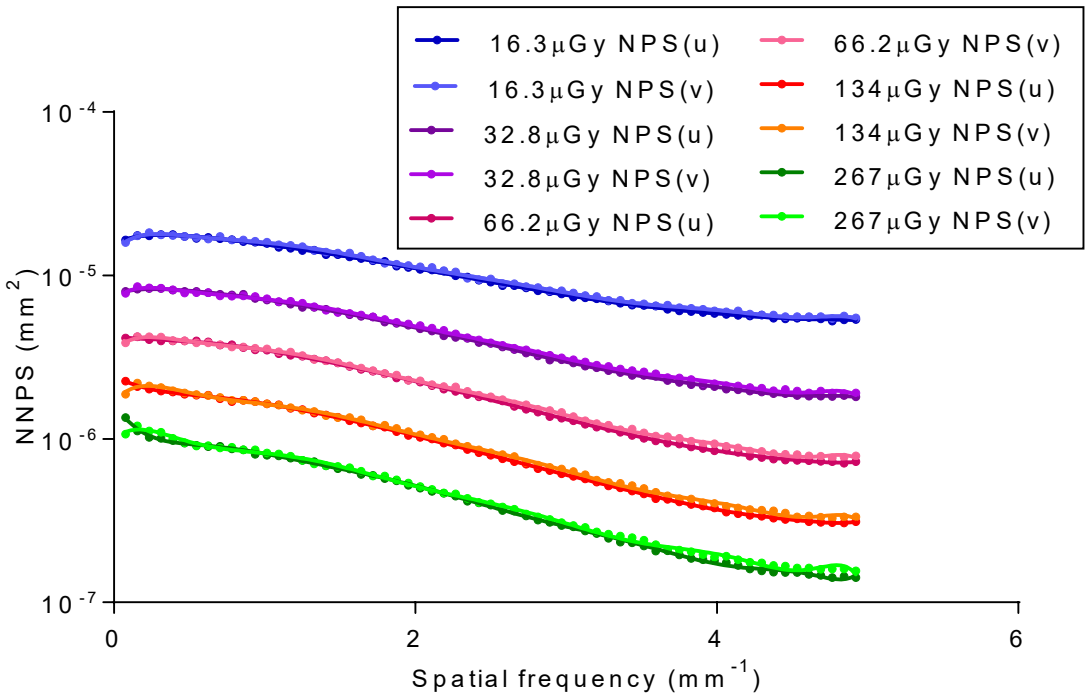


**Figure 18. NNPS curves for a range of air kerma incident to the detector**

Figure 19 shows the DQE averaged in the two orthogonal directions for a range of entrance air kerma. The MTF and DQE measurements were interpolated to show values at standard frequencies in Table 21.

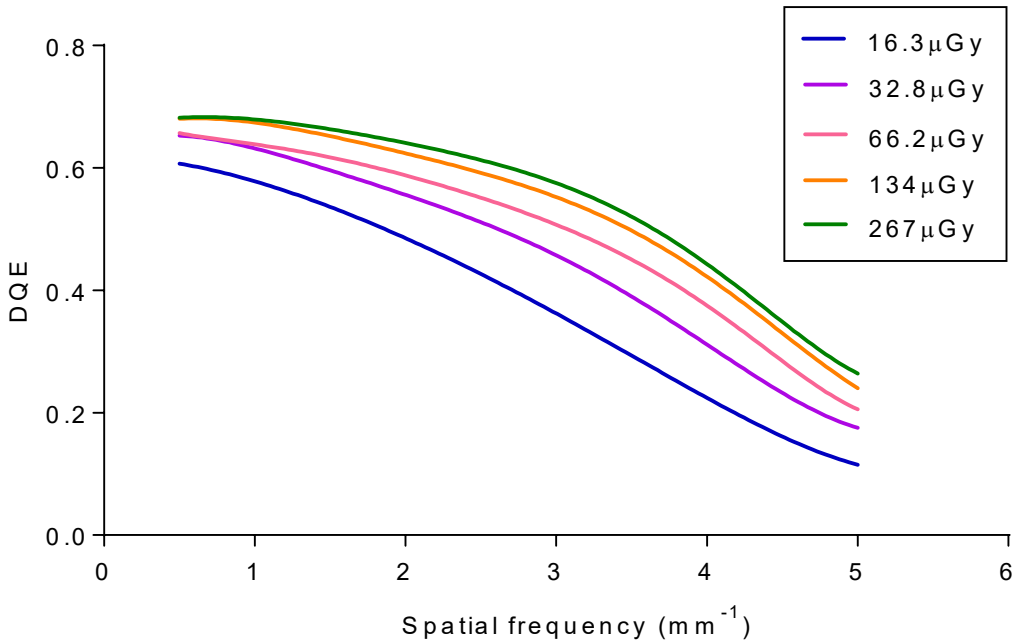


**Figure 19. DQE averaged in both directions for a range of air kerma incident to the detector**

**Table 21. MTF and DQE measurements at standard frequencies (DQE at 66.2µGy)**

| Frequency ($mm^{-1}$) | MTF (u) | MTF (v) | DQE |
|---|---|---|---|
| 0.0 | 1.00 | 1.00 | - |
| 0.5 | 0.92 | 0.92 | 0.68 |
| 1.0 | 0.85 | 0.86 | 0.68 |
| 1.5 | 0.76 | 0.77 | 0.65 |
| 2.0 | 0.65 | 0.67 | 0.63 |
| 2.5 | 0.55 | 0.57 | 0.59 |
| 3.0 | 0.46 | 0.49 | 0.55 |
| 3.5 | 0.38 | 0.41 | 0.50 |
| 4.0 | 0.31 | 0.35 | 0.42 |
| 4.5 | 0.25 | 0.29 | 0.33 |
| 5.0 | 0.20 | 0.23 | 0.24 |

## 3.9 Other tests

The results of all the other tests that were carried out were within acceptable limits as prescribed in the UK protocol[1] and IPEM Report 89.[4]

### 3.9.1 Compression

The measured compressed breast thicknesses are compared with the displayed values in Table 22. They were within 2mm of displayed values. This is well within the IPEM Report 89[4] remedial level of > 5mm.

**Table 22. Indicated compressed breast thickness**

| Actual thickness (mm) | Indicated thickness (mm) | Difference (mm) |
|---|---|---|
| 20 | 18 | 2 |
| 40 | 38 | 2 |
| 70 | 68 | 2 |

Measurements of compression force together with the IPEM Report 89[4] remedial levels are shown in Table 23.

**Table 23. Compression force and thickness**

| | Measured force (N) | IPEM Report 89 remedial level (N) |
|---|---|---|
| Maximum motorised compression | 198 | < 150 or > 200 |
| Maximum compression in any mode | 198 | > 300 |
| Compression change over 30 seconds | 2 | > 20 |

### 3.9.2 Image retention

The image retention factor was 0.01, compared to the NHSBSP upper limit of 0.3.

### 3.9.3 Missed tissue at CWE

The missed tissue was measured as 5mm, which is equal to the NHSBSP limit.

### 3.9.4 Mesh

No discontinuities were seen in the image of the fine wire mesh.

### 3.9.5 Distortion

Measurements showed that there was no distortion in an image of small aluminium balls spaced 50mm apart across the whole image (the tomosynthesis test tool).

### 3.9.6 AEC repeatability

For a series of 5 repeat images, acquired in quick succession, the maximum deviation of mAs from the mean was 1.3%. For 6 images, acquired at intervals over several days of testing, the maximum deviation was 1.9%. The NHSBSP remedial level is 5%.

### 3.9.7 Uniformity and artefacts

Uniformity measurements showed a variation in pixel values of between 2 and 7% relative to the central area of a 24cm x 29cm image of 45mm thick PMMA. The results are shown in Table 24; all are below the NHSBSP remedial level of 10%.

**Table 24. Uniformity**

| Position | Mean pixel value | Deviation from centre value |
|---|---|---|
| Centre | 898 | |
| CWE left corner | 883 | 2% |
| CWE right corner | 884 | 2% |
| Nipple edge left corner | 842 | 6% |
| Nipple edge right corner | 835 | 7% |

There was slight visible non-uniformity in the unprocessed image, as shown in Figure 20. A plot of mean pixel value along the midline, from CWE to nipple edge, is shown in Figure 21.

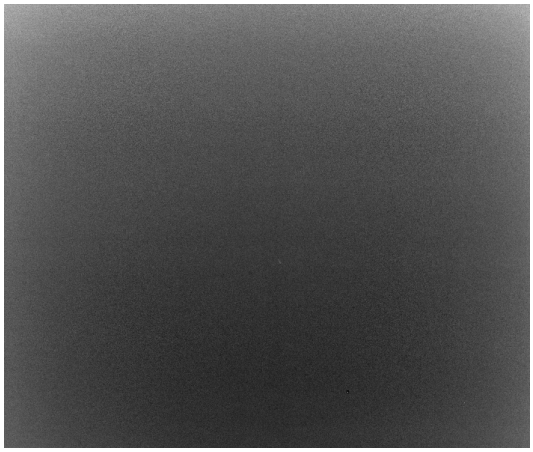

Chest wall edge

**Figure 20. Unprocessed image of 45mm thick PMMA.**

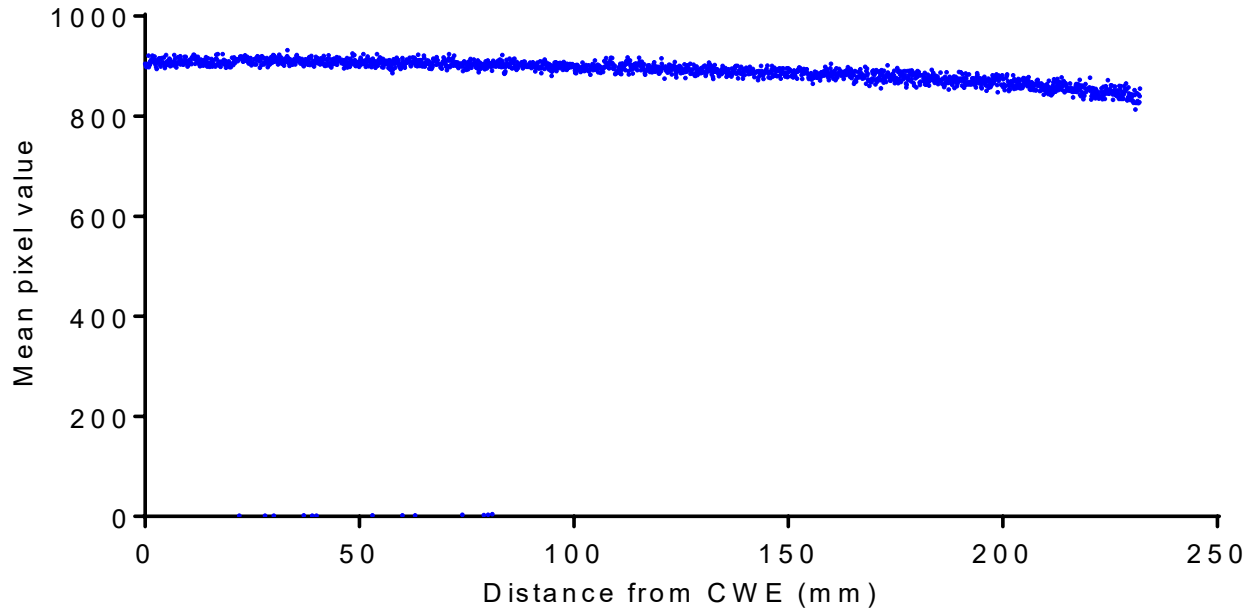


**Figure 21. Profile plot along midline, perpendicular to CWE**

### 3.9.9 Cycle time

For a typical exposure of 34kV Rh/Ag at 28mAs, a subsequent exposure could be made 17 seconds after the start of the previous one.

### 3.9.10 Backup timer

When an AEC exposure was attempted with a steel plate blocking the X-ray beam, the exposure terminated after a short time of less than 1s after the pre-exposure. There was no main exposure and no image acquired. A message “AOP aborted, change acquisition mode” was displayed.

### 3.9.11 Movement and safety

All movements were smooth. The minimum height of the breast support table was 65cm and the maximum was 150cm. There were no rough edges.

A yellow radiation symbol was displayed on the console during exposures.

The safety cut-out (red button) on the console stopped operation when pressed. The display remained on and the system could be rebooted from the console.

# 4. Discussion

The detector response was found to be linear, as expected.

MGDs measured using PMMA were well within the NHSBSP limits for all equivalent breast thicknesses in all 4 AEC modes (Figure 5). The MGDs to a 53mm equivalent breast thickness were 1.19mGy, 0.93mGy, 1.70mGy and 1.70mGy respectively in AEC modes Standard, Dose-, Standard+ and Implant (Tables 7 to 10). The displayed doses were almost all higher than the calculated MGDs, on average by approximately 5%. This may be partly accounted for by small differences in measurement, for example the HVLs in the DICOM headers are 0.37 for 26kV Mo/Mo and 0.57 for 34kV Rh/Ag, slightly different from the measured values in Table 5.

CNR measurements made with plain PMMA showed a steady decrease with increasing equivalent breast thickness (Figure 6). Target CNR values of 10.2 and 15.0, for minimum acceptable and achievable image quality respectively, were calculated. All CNR values exceeded the European limiting values for CNR (Tables 11 to 12). All AEC modes exceeded the CNR target for minimum image quality from 20 to 90mm equivalent breast thicknesses. In the Standard mode the CNR target for achievable image quality was equalled or exceeded up to 60mm equivalent breast thickness. In Standard+ mode this target was exceeded up to 75mm equivalent breast thickness. Consideration should be given to using the Standard mode for breasts up to 60mm thick and the Standard+ mode for greater thicknesses. The Dose- mode is not recommended for routine use because of the resulting reduction in image quality.

The European guidelines include a test for whether the SNR remains approximately constant as the thickness of added PMMA increases. The results (shown in Tables 13 to 15) for Standard, Dose- and Standard+ modes showed that a nearly constant SNR was maintained for total thicknesses of 36mm and above. At 32 and 34mm thickness, a lower SNR value was seen, related to the choice of 26kV Mo/Mo as exposure factors for these thicknesses only. For Implant mode, 34kV Rh/Ag was selected by the AEC for all thicknesses, and no step in SNR value occurred, but there was a gradual decrease with total thickness of PMMA, as shown in Table 16.

However, the test for constant SNR is not the most appropriate test for this system. Since the design aim is to keep CNR constant, rather than SNR, it would be better to modify the test to include a 0.2mm thick aluminium square, and measure CNR instead.

Noise analysis showed that quantum noise is the main contribution to the noise over a wide range of incident air kerma (Figure 10). There are minimal contributions from electronic and structural noise.

Threshold gold thicknesses for a range of detail diameters are shown in Figure 11. At an MGD of 1.26mGy (close to that selected for the equivalent thickness of PMMA in Standard mode), the image quality was very close to the achievable level for all contrast detail diameters.

Threshold gold thickness measurements at different dose levels for the 0.1mm and 0.25mm diameter details were used to calculate MGDs to a simulated 60mm equivalent breast required for the minimum and achievable levels of image quality (Figure 12). This allowed comparisons to be made between this and other systems previously tested. The dose required for the Pristina to reach the achievable level of image quality was comparable to that calculated for other digital mammography systems (Table 20).

The detector performance, as indicated by MTF, NNPS and DQE curves (Figures 17 to 19), was satisfactory.

Results of other miscellaneous tests, presented in Section 3.9, were satisfactory.

# 5. Conclusions

The MGD is well below the remedial level for all AEC modes. In Standard mode, the MGD to the standard breast (53mm equivalent breast) is 1.19mGy. The image quality, as measured by threshold gold thickness, is at the achievable level for the Standard mode.

The GE Senographe Pristina, operating in 2D mode, meets the requirements of the NHSBSP standards for digital mammography systems.

# References


1. Kulama E, Burch A, Castellano I et al. *Commissioning and routine testing of full field digital mammography systems* (NHSBSP Equipment Report 0604, Version 3). Sheffield: NHS Cancer Screening Programmes, 2009

2. van Engen R, Young KC, Bosmans H, et al. European protocol for the quality control of the physical and technical aspects of mammography screening. In *European guidelines for quality assurance in breast cancer screening and diagnosis*, Fourth Edition. Luxembourg: European Commission, 2006

3. van Engen R, Bosmans H, Dance D et al. Digital mammography update: European protocol for the quality control of the physical and technical aspects of mammography screening. In *European guidelines for quality assurance in breast cancer screening and diagnosis,* Fourth edition – Supplements. Luxembourg: European Commission, 2013

4. Moore AC, Dance DR, Evans DS et al. *The Commissioning and Routine Testing of Mammographic X-ray Systems.* York: Institue of Physics and Engineering in Medicine, Report 89, 2005

5. Alsager A, Young KC, Oduko JM. Impact of heel effect and ROI size on the determination of contrast-to-noise ratio for digital mammography systems. In *Proceedings of SPIE Medical Imaging*, Bellingham WA: SPIE Publications, 2008, 691341: 1-11

6. Boone JM, Fewell TR and Jennings RJ. Molybdenum, rhodium and tungsten anode spectral models using interpolating polynomials with application to mammography *Medical Physics,* 1997, 24: 1863-1974

7. Berger MJ, Hubbell JH, Seltzer SM, Chang et al. XCOM: Photon Cross Section Database (version 1.3) http://physics.nist.gov/xcom (Gaithersburg, MD, National Institute of Standards and Technology), 2005

8. Young KC, Oduko JM, Bosmans H, Nijs K, Martinez L. Optimal beam quality selection in digital mammography. *British Journal of Radiology*, 2006, 79: 981-990

9. Young KC, Cook JH, Oduko JM. Automated and human determination of threshold contrast for digital mammography systems. In *Proceedings of the 8th International Workshop on Digital Mammography,* Berlin: Springer-Verlag, 2006, 4046: 266-272

10. Young KC, Alsager A, Oduko JM et al. Evaluation of software for reading images of the CDMAM test object to assess digital mammography systems. In *Proceedings of SPIE Medical Imaging*, Bellingham WA: SPIE Publications, 2008, 69131C: 1-11

11. IEC 62220-1-2, *Determination of the detective quantum efficiency – Detectors used in mammography.* International Electrotechnical Commission, 2007

12. Mackenzie A, Oduko JM. *Technical evaluation of the Hologic 3Dimensions digital mammography system in 2D mode.* London: Public Health England, 2019

13. Young KC, Oduko JM, Gundogdu O and Asad M. *Technical evaluation of profile automatic exposure control software on GE Essential FFDM systems* (NHSBSP Equipment Report 0903). Sheffield: NHS Cancer Screening Programmes, 2009

14. Tyler N, Mackenzie A. *Technical evaluation of Siemens Revelation Digital Mammography System in 2D mode.* London: Public Health England, 2019

15. Oduko JM, Young KC. *Technical evaluation of Philips MicroDose L30 with AEC software version 8.3* (NHSBSP Equipment Report 1305). Sheffield: NHS Cancer Screening Programmes, 2013

16. Strudley CJ, Oduko JM, Young KC. *Technical evaluation of the Fujifilm AMULET Innovality Digital Mammography System* (NHSBSP Equipment Report 1601). London: Public Health England, 2017

17. Tyler N, Young KC, Oduko JM, Mackenzie A. *Technical evaluation of IMS Giotto Class Digital Mammography System in 2D mode.* London: Public Health England, 2019

18. Tyler N, Oduko JM, Strudley C, Mackenzie A. *Technical evaluation of planmed Clarity Digital Mammography System in 2D mode.* London: Public Health England, 2019